VII International Conference on Computational Methods for Coupled Problems in Science and Engineering
COUPLED PROBLEMS 2017
M. Papadrakakis, E. Oñate and B. Schrefler (Eds)

EVALUATION OF LINEAR AND QUADRATIC MODAL ANALYSIS FOR A PARTITIONED FSI SOLVER

Alfred E.J. Bogaers*, Oliver F. Oxtoby†, Johan A. Heyns†, Ridhwaan Suliman† and Louw H. van Zyl†

* Advanced Mathematical Modelling, Modelling and Digital Sciences, CSIR, South Africa
email: abogaers@csir.co.za

†Aeronautic Systems, Defence Peace Safety and Security, CSIR, South Africa

Key words: fluid-structure interactions, partitioned, modal analysis, quadratic mode shape components

Abstract. In this paper, linear and quadratic modal approximations of elastodynamic solid deformation in FSI problems are considered. Firstly, the theory of quadratic extension of modal analysis presented in [1] is laid out. The quadratic and linear approximations are then benchmarked against full FEM analysis in various test cases. These are chosen to be representative of flutter considerations in the aerospace field. The quadratic approximation is shown to produce a markedly better prediciton of solid deformation for small to medium deflections.

1 INTRODUCTION

Accurately predicting the onset of flutter is an important consideration when designing and certifying aircraft for an intended flight envelope. It is by now common practice in computational aeroelasticity to approximate the structural deformation using normal linear modal analysis [2, 3]. Linear modal analysis provides an efficient approximation for aeroelastic applications, and has been shown to provide credible flutter predictions [4]. The structural response is described by the system mode shapes and associated natural frequencies, which can either be obtained from experimental ground vibration tests (GVTs) or be approximated numerically using techniques such as the finite element method.

Linear modal dynamic systems are however limited to very small deflections, and are incapable of providing accurate representations for large rotations (for example when performing T-tail flutter analysis [5]). To improve the accuracy of modal analysis for rotating reference frames, Segelman *et al.* [6] introduced the method of quadratic mode shape components.

We aim to demonstrate via examples that these quadratic mode shape components provide an approximation of the geometric non-linearity present within the full elasto-dynamic structural equations, albeit for relatively small deflections. The addition of the quadratic mode shape terms remain a linearised expansion, and therefore retains much of the numerical efficiency offered by normal modal analysis.

Following the work presented in [1], we will outline the procedure for approximating the quadratic mode shape components using a number of static, small strain finite element analyses. The improved accuracy offered by including the quadratic terms will be shown on a number of fluid-structure interactions (FSI) benchmark problems, and compared to high-fidelity FSI simulations.

2 Modal Dynamics

2.1 Linear Modal Dynamics

Using standard FEM analysis software (and to a lesser extent FVM), it is possible to compute the eigenvectors or mode shapes ϕ_i along with the natural frequencies ω_i of a given linear elastic structure. The real space displacement $\boldsymbol{u}$ can then be approximated by the linear expansion of the mode shapes such that

$$\boldsymbol{u} = \sum_{i=1}^{n} q_i \phi_i \tag{1}$$

where q_i are the modal expansion coefficients or modal variables, and n is the number of retained mode shapes. The generalised equation for aeroelastic structural deformation rewritten in terms of the of the modal variables can be expressed as

$$\boldsymbol{M}\ddot{q} + \boldsymbol{C}\dot{q} + \boldsymbol{K}q = Q \tag{2}$$

where $\boldsymbol{M}$, $\boldsymbol{K}$ and $\boldsymbol{C}$ represents the reduced mass, stiffness and damping matrices. Q represents the generalised force vector given by

$$Q_i = \int_{\Omega} d\boldsymbol{F}\phi_i, \tag{3}$$

where $d\boldsymbol{F} = p\boldsymbol{n_f}dA - \boldsymbol{\sigma}\cdot\boldsymbol{n}_f dA$ is the nodal forces along the FSI interface. Here p represents the interface pressure, and $\boldsymbol{\sigma_f}$ the fluid viscous stress tensor and $\boldsymbol{n_f}dA$ the outward pointing surface area normal vector. Typically ϕ_i is interpolated from the structural mesh to the fluid domain interface mesh, where $d\boldsymbol{F}$ then represents the nodal forces acting along the fluid domain's interface. This allows for the generalised forces, Q, and the general elastic equation (2) to be directly computed along the fluid interface.

When computed using the FEM, the mode shapes and elastic equation (2) are typically normalised such that the reduced stiffness and damping matrices become

$$\boldsymbol{M} = \boldsymbol{I} \quad \text{and} \quad \boldsymbol{K} = \text{diag}\left[\omega_n^2\right]. \tag{4}$$

2.2 Quadratic mode shape components

For small displacements, van Zyl *et al.* [1] demonstrated that the linearised expansion in equation (1) can be improved by including coupled quadratic mode shape components ϕ_{ij} such that

$$\boldsymbol{u} = \sum_{i=1}^{n} q_i \phi_i + \sum_{i=1}^{n} \sum_{j=1}^{n} q_i q_j \phi_{ij}. \tag{5}$$

Given the quadratic mode shape components, the generalised force Q_i is now defined as

$$Q_i = \int_{\Omega} d\boldsymbol{F} \cdot \left(\phi_i + \sum_{j=1}^{n} q_j \phi_{ij} \right). \tag{6}$$

The generalised structural equation (2) can be rewritten as

$$M_{ij}\ddot{q}_j + C_{ij}\dot{q}_j + \tilde{K}_{ij} q_j = \tilde{Q}_i, \tag{7}$$

where $\tilde{K}_{ij} = K_{ij} - \int_{\Omega} d\boldsymbol{F} \cdot \phi_{ij}$ and $\tilde{Q}_i = \int_{\Omega} d\boldsymbol{F} \cdot \phi_i$. The linear system (7) is solved at every time step using fourth-order Runge-Kutta integration.

3 APPROXIMATING QUADRATIC MODE SHAPE COMPONENTS FROM FEM

Following the work presented in [1], the quadratic mode shape components can be approximated using a number of static, small strain, linear elastic FEM analyses. This as opposed to [6, 7, 8] which require multiple non-linear static analyses. The method was first proposed using energy arguments derived using truss elements, and later extended to general elastic finite elements.

For the discussion to follow, assume we have available two linear mode shapes, namely ϕ_i and ϕ_j. A linearised approximation for the displacement of node l, of a general elastic element, can then be given as

$$\boldsymbol{u}^l = q_i \phi_i^l + q_j \phi_j^l + \boldsymbol{u}_R \tag{8}$$

where $\boldsymbol{u}_R$ represents an additional rotational displacement term not accounted for by linear modal analysis. The aim of the additional higher order quadratic mode shape components is to counteract the effect of neglecting $\boldsymbol{u}_R$. Given two mode shapes, the additional rotational components can be approximated following [1] as

$$\begin{aligned} \boldsymbol{u}_R &= \boldsymbol{u}_R^{ii} + \boldsymbol{u}_R^{jj} + \boldsymbol{u}_R^{ij}. \\ &= \frac{1}{2} q_i^2 \boldsymbol{R}_i \times \left(\boldsymbol{R}_i \times \boldsymbol{p}^l \right) + \frac{1}{2} q_j^2 \boldsymbol{R}_j \times \left(\boldsymbol{R}_j \times \boldsymbol{p}^l \right) + \frac{1}{4} q_i q_j \left[\boldsymbol{R}_i \times \left(\boldsymbol{R}_j \times \boldsymbol{p}^l \right) + \boldsymbol{R}_j \times \left(\boldsymbol{R}_i \times \boldsymbol{p}^l \right) \right] \end{aligned} \tag{9}$$

Here $\boldsymbol{p}^l$ is a position vector from some point within the element to node l. The exact location of point p is insignificant and can be taken to be element centroid or the average of the nodal co-ordinates. Vectors $\boldsymbol{R}_i$ and $\boldsymbol{R}_j$ are the rigid body rotations associated with mode shapes ϕ_i and ϕ_j respectively for a given element.

In equation (9), the first term, $\frac{1}{2}q_i^2\boldsymbol{R}_i \times \left(\boldsymbol{R}_i \times \boldsymbol{p}^l\right)$, relates to the quadratic component to be cancelled by ϕ_{ii}, the second with ϕ_{jj} and the third with the coupled quadratic mode shape component $\phi_{ij} = \phi_{ji}$. In general, because of the symmetry $\phi_{ij} = \phi_{ji}$, for n linear mode shapes, there will be $(n+3)\,n/2 - n$ quadratic mode shape components to be computed for, i.e.

$$\boldsymbol{\phi}^{ii} = \{\phi_{11}, \phi_{12}, \phi_{1N}, \phi_{22}, \phi_{23}, ...\phi_{2n}, ..., \phi_{nn}\}\,.$$

Computation of the various components of $\boldsymbol{u}_R$ requires isolating the various rigid body rotation vectors, $\boldsymbol{R}_{i,j}$, associated with each of the linear mode shapes $\phi_{i,j}$. Consider Figure 1, where each mode shape is expressed as a displacement vector represented by the summation of rigid body translation and rigid body rotation

$$\{\boldsymbol{\phi}_i\}_{el} = \boldsymbol{T}_{el} + \boldsymbol{R}_{i,el} \times \boldsymbol{p}, \tag{10}$$

where $\boldsymbol{T}_{el} = \{t_x, t_y, t_z\}$ represents the linear translation components and $\boldsymbol{R}_{i,el} = \{r_x, r_y, r_z\}$ the rigid body rotation (angles of rotation) for the given element. The system described by (10) is however over determined, since there are only 6 unknowns to be solved for but $3m$ known components of $\phi_i = \{\phi_{1,x}, \phi_{1,y}, \phi_{1,z}, ..., \phi_{m,z}\}^T$, where m is the number of nodes within the element. The least squares problem to approximate the rigid body rotation vector $\boldsymbol{R}_i$ associated with mode shape ϕ_i for an m noded element can be expressed in matrix form as

$$\begin{bmatrix} \boldsymbol{I} & \boldsymbol{P}_1 \\ \boldsymbol{I} & \boldsymbol{P}_2 \\ \vdots & \vdots \\ \boldsymbol{I} & \boldsymbol{P}_m \end{bmatrix} \begin{Bmatrix} t_x \\ t_y \\ t_z \\ r_x \\ r_y \\ r_z \end{Bmatrix} = \begin{Bmatrix} \phi_{1,x} \\ \phi_{1,y} \\ \phi_{1,z} \\ \vdots \\ \phi_{m,x} \\ \phi_{m,y} \\ \phi_{m,z} \end{Bmatrix}, \tag{11}$$

where $\boldsymbol{P}_l$ is a matrix representative of the cross product between the reference vector associated with node l and the to be computed rotation vector, $\boldsymbol{p}_l^T \times \boldsymbol{R}_i$, i.e.

$$\boldsymbol{P}_l = \begin{bmatrix} 0 & p_{l,z} & -p_{l,y} \\ -p_{l,z} & 0 & p_{l,x} \\ p_{l,y} & -p_{l,x} & 0 \end{bmatrix}, \quad \text{and} \quad \boldsymbol{I} = \begin{bmatrix} 1 & 0 & 0 \\ 0 & 1 & 0 \\ 0 & 0 & 1 \end{bmatrix}. \tag{12}$$

There will be a rotation vector for each element within the structural mesh, for each of the linear mode shapes.

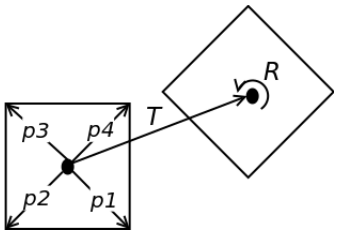

Figure 1: An exaggerated illustration of the translation, $\boldsymbol{T}$, and rotation, $\boldsymbol{R}$, of a two-dimensional 4-noded element.

The quadratic mode shape components $\sum_{i=1}^{N}\sum_{j=1}^{N} q_i q_j \boldsymbol{\phi}_{ij}$ need to cancel out the additional rotational displacement term $\boldsymbol{u}_R$. From a kinetic energy perspective, as explained in [1], in order to minimise spurious contributions to the kinetic energy, the quadratic mode shape components should be orthogonal to the corresponding linear mode shapes. A convenient means is to orthogonalise the linear and quadratic mode shapes with respect to the system stiffness matrix

$$\boldsymbol{\phi}_i^T \left[K\right] \boldsymbol{\phi}_{ii} = 0, \tag{13}$$

where $[K]$ here represents the full FEM, static, small strain stiffness matrix, and not the reduced modal stiffness matrix.

There are therefore two conditions to be satisfied. The quadratic modes shapes need to be orthogonal to the linear mode shapes and need to cancel out the effects of the additional rotational term $\boldsymbol{u}_R$.

The rotational terms are cancelled by computing the reaction forces resulting from the displacement $\boldsymbol{u}_R$, and subsequently computing the equivalent displacement which would cancel out the the reaction forces. Given the rotational displacement $\boldsymbol{u}_R$, the reaction can be computed for a given element as

$$\boldsymbol{f}^i_{\text{el}} = \left[K\right]_{\text{el}} \boldsymbol{u}^i_{R,\text{el}}, \tag{14}$$

where $\left[K\right]_{\text{el}}$ represents the local element stiffness matrix. Using the appropriate global degrees of freedom, the forces should be appropriately summed into the global force vector $\boldsymbol{f}^i_{\text{global}}$. ϕ_{ii} can then be computed by solving the general FEM linear system of

$$\left[K\right] \boldsymbol{\phi}_{ii} = \boldsymbol{f}^i_{\text{global}}. \tag{15}$$

In order to satisfy both the orthogonality constraint (13) along with (15) a Lagrange multiplier system of equations can be constructed and solved for

$$\begin{bmatrix} [K] & [K]\,\boldsymbol{u}^i_R \\ \boldsymbol{u}^{i^T}_R\,[K] & \mathbf{0} \end{bmatrix} \begin{Bmatrix} \boldsymbol{\phi}_{ii} \\ \lambda \end{Bmatrix} = \begin{Bmatrix} \boldsymbol{f}^i \\ 0 \end{Bmatrix}. \tag{16}$$

Similarly, the coupled quadratic modes $\boldsymbol{\phi}^{ij}$ have two orthogonality conditions which have

to be satisfied

$$\begin{bmatrix} [K] & [K]\,\boldsymbol{u}_R^i & [K]\,\boldsymbol{u}_R^j \\ \boldsymbol{u}_R^{iT}\,[K] & 0 & 0 \\ \boldsymbol{u}_R^{jT}\,[K] & 0 & 0 \end{bmatrix} \begin{Bmatrix} \boldsymbol{\phi}_{ij} \\ \lambda_1 \\ \lambda_2 \end{Bmatrix} = \begin{Bmatrix} \boldsymbol{f}^{ij} \\ 0 \\ 0 \end{Bmatrix}. \tag{17}$$

The procedure to approximate the quadratic mode shape components can be summarised as follows:

1. Using a standard FEM package solve for the set of linear mode shapes $\boldsymbol{\phi} = \{\phi_1, ..., \phi_N\}$.
2. For each element compute a reference point p, and compute the corresponding reference vector $\boldsymbol{p}^l$ for each node l.
3. For each of the retained mode shapes $\boldsymbol{\phi}_i$, compute the associated element solid body rotation vector $\boldsymbol{R}^i_{\text{el}}$ by solving the least squares problem (11).
4. Using (9), compute each component of $\boldsymbol{u}^{ij}_{\text{el},R}$.
5. Compute the nodal reaction forces $\boldsymbol{f}^{ij}_{\text{el}} = [K]_{\text{el}}\,\boldsymbol{u}^{ij}_{\text{el},R}$.
6. Sum up $\boldsymbol{f}^{ij}_{\text{el}}$ into the appropriate global force vector $\boldsymbol{f}^i_{\text{global}}$.
7. Solve for the approximate $\boldsymbol{\phi}^{ii}$ and $\boldsymbol{\phi}^{ij}$ components using either (16) or (17) depending on whether there are one or two orthogonality conditions that need to be satisfied.

4 VALIDATING MODAL FSI AGAINST FULL HIGH-FIDELITY FSI

In this section we aim to compare the approximations obtained using linear and quadratic mode shapes and compare these to results obtained using full, high-fidelity FSI simulations. The same spatial and temporal discretisation will be used for both the high-fidelity and modal based ROM. This in turn allows for a direct comparison of the methods, as both sets of simulations will have the same numerical errors.

The normal linear mode shapes and natural frequencies are computed using CalculiX [9]. The fluid flow is computed using OpenFOAM [10], and the fluid and structural domains are implicitly coupled using Aitken's method. The full, high-fidelity FSI simulations are performed using an implicit, partitioned coupling of OpenFOAM and CalculiX [11].

In all test cases, we retain the first 4 linear mode shapes, which corresponds to 10 additional quadratic mode shape components.

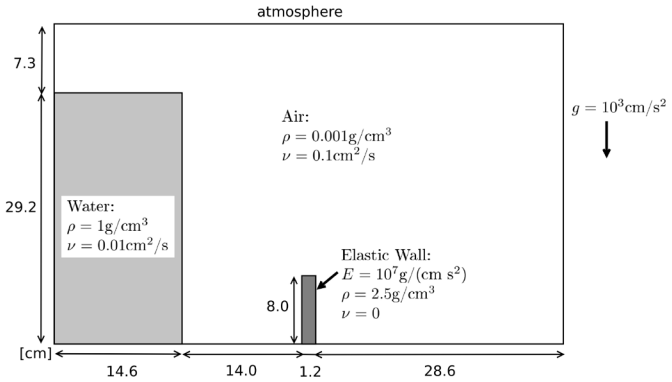

Figure 2: Dam break with elastic structure problem description.

4.1 Dam Break VOF validation

We consider here a simple dam break problem, where a collapsing column of water strikes a flexible elastic structure, which has previously been analysed in [12, 13, 14]. The problem setup is shown in Figure 2, and consists of a 29.2cm column of water which collapses under gravity, striking an 8cm tall, 1.2cm wide, elastic obstacle. The tank is open at the top, and surface tension effects are ignored due to the large length scales.

The problem is solved here using 3672 linear FVM elements and 14 quadratic, full integration solid elements. The time step size is chosen as Δt =0.001s. In Figure 3, the advancing front along with the elastic deformation is shown for various time steps.

A comparison of the tip displacement of the flexible baffle is shown in Figure 4. The improvement in solution accuracy offered by the inclusion of the quadratic mode shape components is directly evident.

4.2 T-Tail

A T-tail like structure is analysed here under fluid cross-flow for 3 different inlet velocities of 1m/s, 3m/s and 5m/s. The problem is selected to illustrate the improved accuracy offered by the quadratic mode shape components when considering larger structural deformations, and problems with rotating reference frames. The geometry along with material properties is outlined in Figure 5. The aim is to provide a preliminary indication of the modal FSI solver using quadratic mode shapes for different deformation magnitudes.

In Figure 6 the T-tail deformations along with pressure contours is shown for the different inlet velocities (computed using the high-fidelity FSI solver) with a comparison of the tip displacements shown in Figure 7. The improvement offered by the inclusion of the additional quadratic mode shape components are once again visible at higher flow rates. The problem clearly highlights, that while the quadratic modes do provide improved accuracy, the applicability remains limited to comparatively small displacements.

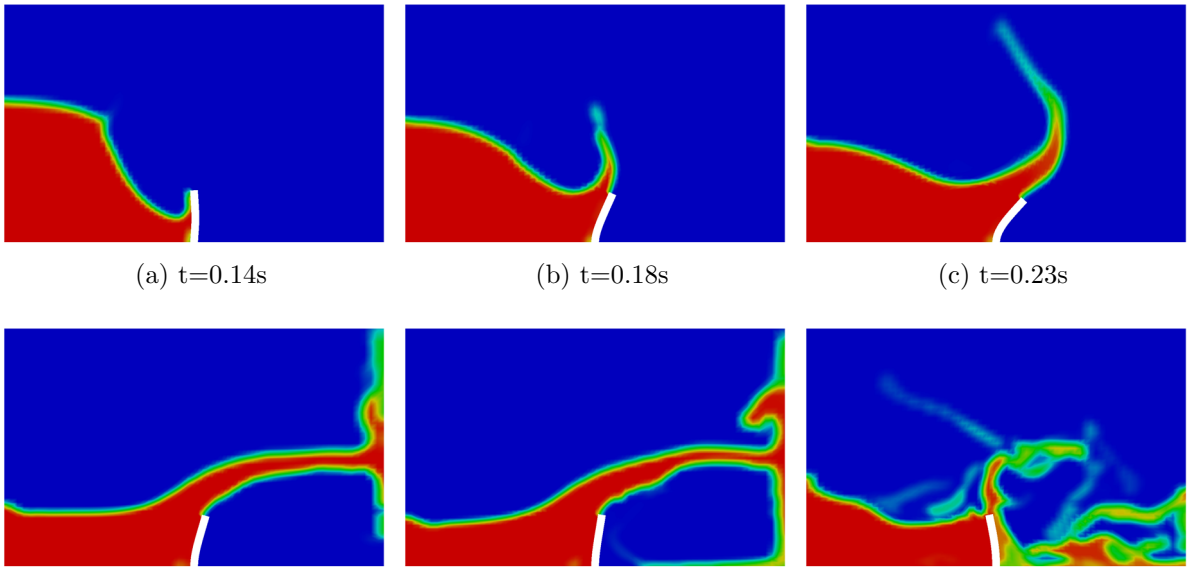

(a) t=0.14s (b) t=0.18s (c) t=0.23s

(d) t=0.38s (e) t=0.46s (f) t=0.8s

Figure 3: Wave interaction with elastic obstruction at various time steps.

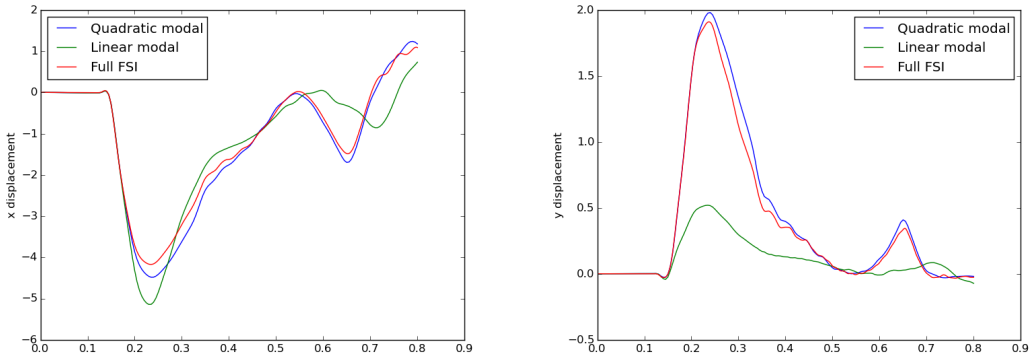

(a) (b)

Figure 4: Comparison of the displacement using linear and quadratic modal dynamics with full high-fidelity FSI. A total of 4 modes are used for the modal dynamics analysis.

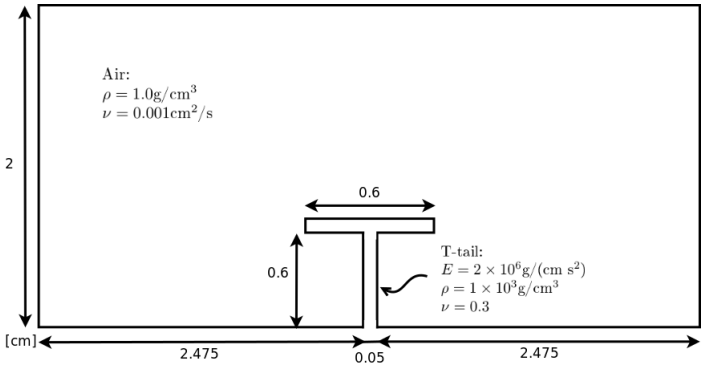

Figure 5: T-Tail material properties and problem description.

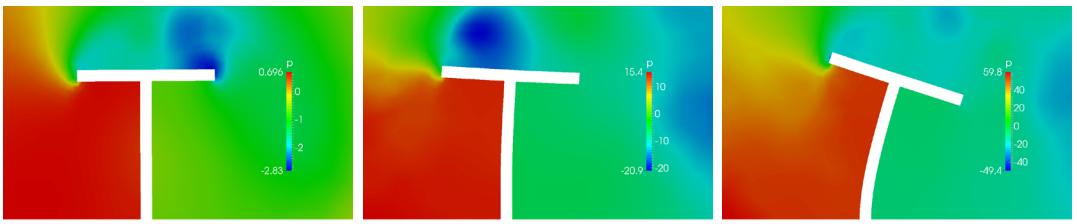

(a) (b) (c)

Figure 6: Pressure contours along with structural deformation at $t = 1.5s$ for inlet velocities of (a) 1m/s, (b) 3m/s and (c) 5m/s.

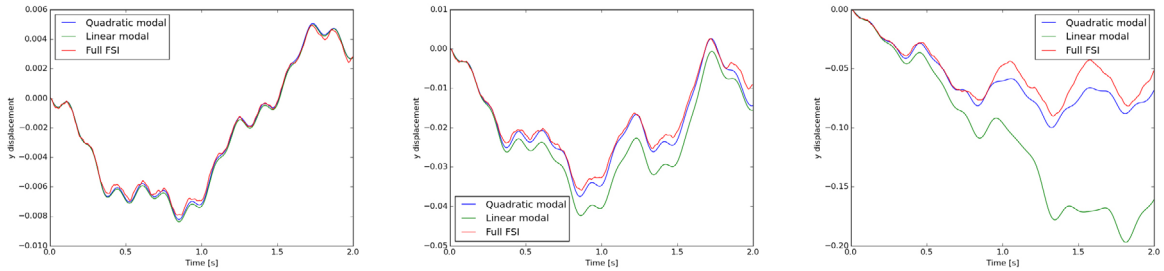

(a) (b) (c)

Figure 7: Comparison of tip y-displacement for inlet velocities of (a) 1m/s, (b) 3m/s and (c) 5m/s. 4 mode shapes are retained for the modal analysis.

Table 1: Comparison of the beam tip frequency of oscillations, compared to the results obtained in [15].

Frequency [Hz]	Linear Modal	Quadratic Modal	Full FSI	Results from [15]
u_x	0.0	3.0	3.72	3.8
u_y	1.85	1.88	1.9	2.0

5 2D flexible beam

In this test problem, flow around a fixed cylinder with an attached flexible beam is analysed. The beam undergoes large deformations induced by oscillating vortices formed by flow around the circular bluff body.

The problem was first proposed by Turek *et al.* [15], and has received substantial numerical verification. The problem layout and material properties are provided in Figure 8(a).

The FSI problem consists of a 0.02m thick, 0.35m long flexible beam, attached to a fixed cylinder with diameter of 0.1m. The cylinder centre is by design constructed to be non-symmetric to remove dependence on numerical errors to induce the onset of deformations. A parabolic inlet boundary condition, with mean flow velocity of $\bar{U} = 1\text{m/s}$ is slowly ramped up for $t < 0.5\text{s}$ via $(1 - \cos(\pi t/2))/2$. The top, bottom and fixed cylinder walls are defined as non-slip boundaries. The problem is solved here using 3800 finite-volume fluid cells, and 72 full integration, bi-quadratic finite elements, with a time step size of $\Delta t = 0.001\text{s}$.

A snapshot of the beam deformation based on the full FSI simulation is shown in Figure 8(b) with a comparison of the beam tip displacements in Figures 8(c) and 8(d). Both the linear and quadratic modal analysis correctly predicts the state of flutter, but are incapable of correctly computing the magnitudes of the oscillating beam. The computed oscillation frequencies is summarised in Table 1. The frequencies computed using both the linear and quadratic mode shapes compare favourably.

6 CONCLUSION

In this study we set out to directly compare linear and quadratic modal analysis on a set of FSI benchmark problems. The procedure to compute the quadratic components using a number of small strain FEM analysis was outlined. Approximating the structural deformation using the quadratic mode shape components adds only a mild additional complexity, retains the numerical efficiency offered by normal linear modal analysis, all the while offering noticeably improved accuracy (albeit still limited to comparatively small structural deformations).

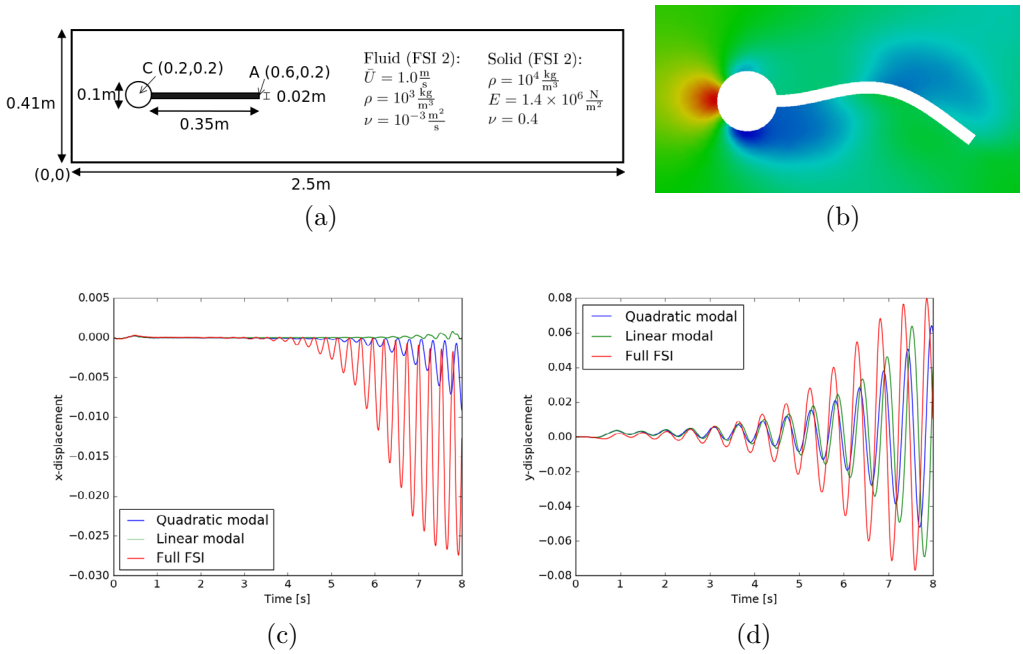

Figure 8: (a) Flexible beam problem description, (b) with a snapshot of the beam displacement and pressure using full, high-fidelity FSI, with a comparison of the beam tip (c) x-displacement and (d) y-displacement.

REFERENCES

[1] Van Zyl, L. & Mathews, E. Quadratic mode shape components from linear finite element analysis. *Journal of Vibration and Acoustics* **134**, 014501 (2012).

[2] Kamakoti, R. & Shyy, W. Fluid–structure interaction for aeroelastic applications. *Progress in Aerospace Sciences* **40**, 535–558 (2004).

[3] Schuster, D. M., Liu, D. D. & Huttsell, L. J. Computational aeroelasticity: success, progress, challenge. *Journal of Aircraft* **40**, 843–856 (2003).

[4] Debrabandere, F., Tartinville, B. & Hirsch, C. A staggered method using a modal approach for fluid-structure interaction computation. In *Proceedings of the 15 th International Forum on Aeroelasticity and Structural Dynamics* (2011).

[5] Van Zyl, L. H. & Mathews, E. H. Aeroelastic analysis of T-tails using an enhanced doublet lattice method. *Journal of Aircraft* **48**, 823–831 (2011).

[6] Segalman, D. & Dohrmann, C. A method for calculating the dynamics of rotating flexible structures, Part 1: Derivation. *Journal of Vibration and Acoustics* **118**, 313–317 (1996).

[7] Dohrmann, C. & Segalman, D. Use of quadratic components for buckling calculations. *Journal of sound and vibration* **208**, 339–344 (1997).

[8] Segalman, D., Dohrmann, C. & Slavin, A. A method for calculating the dynamics of rotating flexible structures, Part 2: Example calculations. *Journal of vibration and acoustics* **118**, 318–322 (1996).

[9] Dhondt, G. Calculix crunchix user's manual version 2.5 (2007).

[10] OpenFOAM: The open source CFD toolbox user guide, version 2.1.0 (2010).

[11] Bogaers, A., Kok, S., Reddy, B. & Franz, T. Quasi-Newton methods for implicit black-box FSI coupling. *Computer Methods in Applied Mechanics and Engineering* **279**, 113–132 (2014).

[12] Kassiotis, C. *Nonlinear fluid-structure interaction: a partitioned approach and its application through component technology.* Ph.D. thesis, Université Paris-Est (2009).

[13] Walhorn, E., Kölke, A., Hübner, B. & Dinkler, D. Fluid–structure coupling within a monolithic model involving free surface flows. *Computers & structures* **83**, 2100–2111 (2005).

[14] Bogaers, A., Kok, S., Reddy, B. & Franz, T. An evaluation of Quasi-Newton methods for application to FSI problems involving free surface flow and solid body contact. *Computers & Structures* **173**, 71–83 (2016).

[15] Turek, S. & Hron, J. *Proposal for numerical benchmarking of fluid-structure interaction between an elastic object and laminar incompressible flow* (Springer, 2006).